Supporting Information

Toward highly efficient bifunctional electrocatalysts for zinc-air battery: From theoretical prediction to ternary FeCoNi design

Wenhao Tang [a], Jialin He [c], Kewei Teng [b], Lei Gao [c], Ruiyu Qi [b], Yirui Deng [a], Ruiping Liu [a, b, *], Ang Li [d], Huadong Fu [c, *], Chang-an Wang [e, *]

[a] School of Chemical & Environmental Engineering, China University of Mining and Technology (Beijing), Beijing 100083, P. R. China

[b] Department of Materials Science and Engineering, China University of Mining and Technology (Beijing), Beijing 100083, P. R. China

[c] Institute for Advanced Materials and Technology, University of Science and Technology Beijing, Beijing 100083, P. R. China

[d] Beijing Key Laboratory of Microstructure and Property of Advanced Materials, Beijing University of Technology, Beijing 100124, P. R. China

[e] State Key Laboratory of New Ceramics and Fine Processing, School of Materials Science and Engineering, Tsinghua University, Beijing 100084, P. R. China

*Corresponding authors. E-mail:

Prof. R. P. Liu, E-mail: lrp@cumtb.edu.cn.

Prof. H. D. Fu, E-mail: hdfu@ustb.edu.cn.

Prof. C. A. Wang, Email: wangca@mail.tsinghua.edu.cn.

1. Supplementary Figures

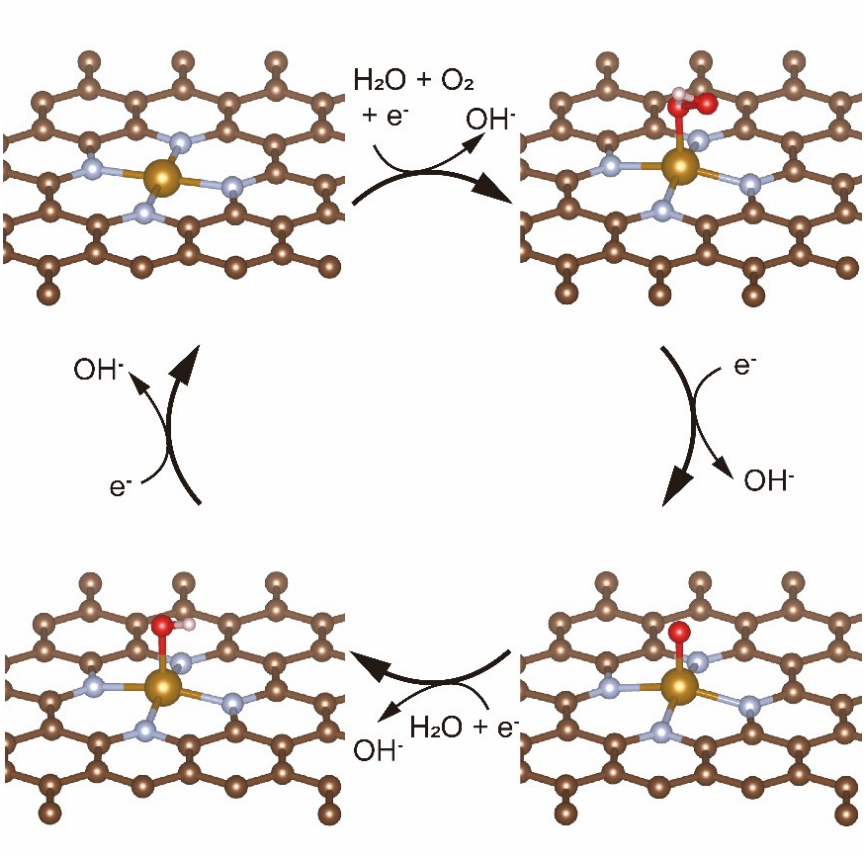

Fig. S1 The mechanism of $4e^-$ ORR in alkaline medium occurring on the Fe atom single-site of Fe-N_4.

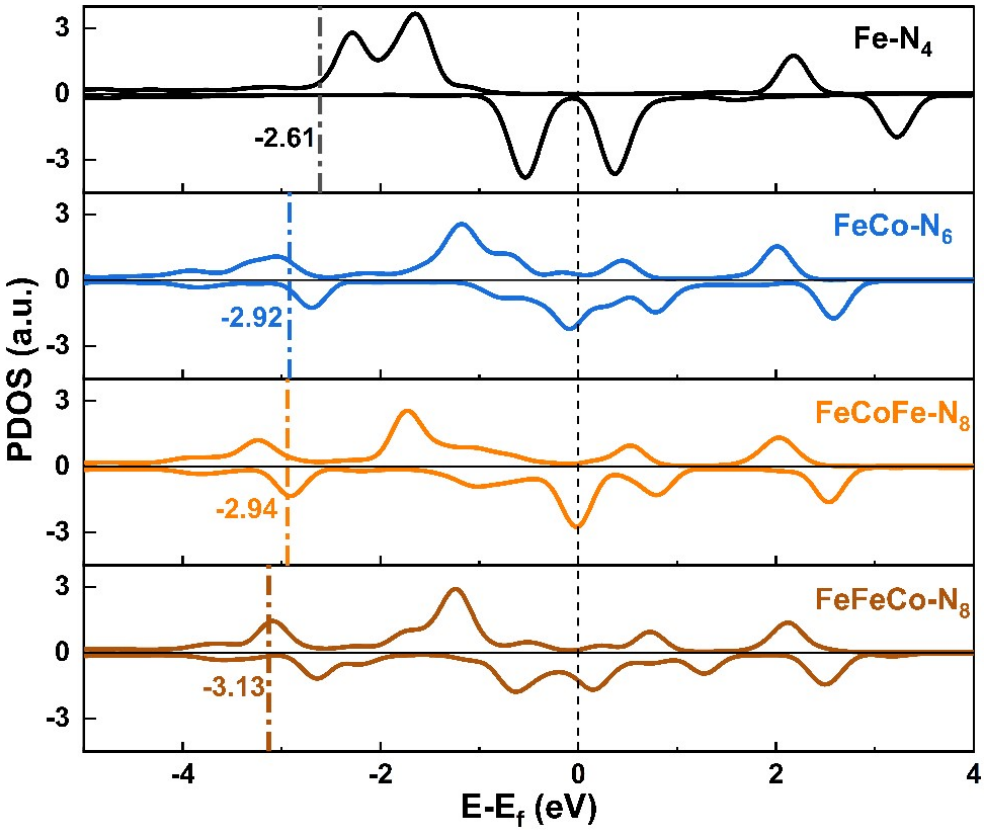

Fig. S2 The partial density of states (PDOSs) of Fe-3d orbitals in Fe-N_4, FeCo-N_6, FeCoFe-N_8 and FeFeCo-N_8.

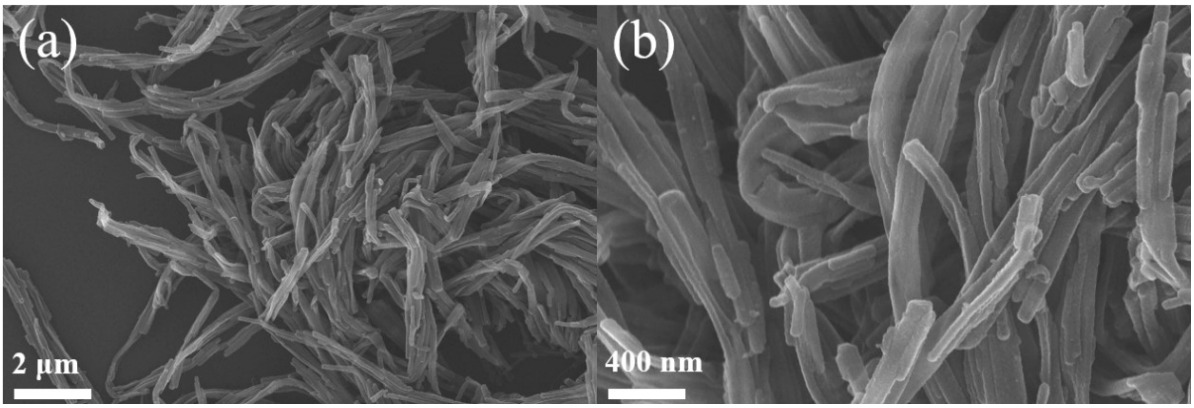

Fig. S3 SEM images of PPy-NTs.

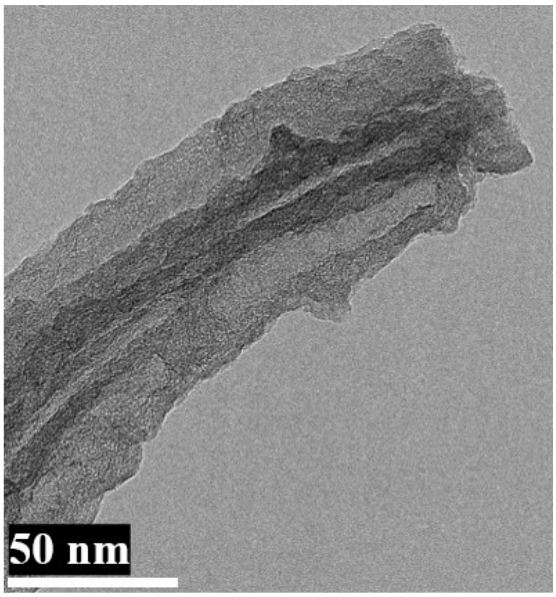

Fig. S4 TEM image of hNCTs.

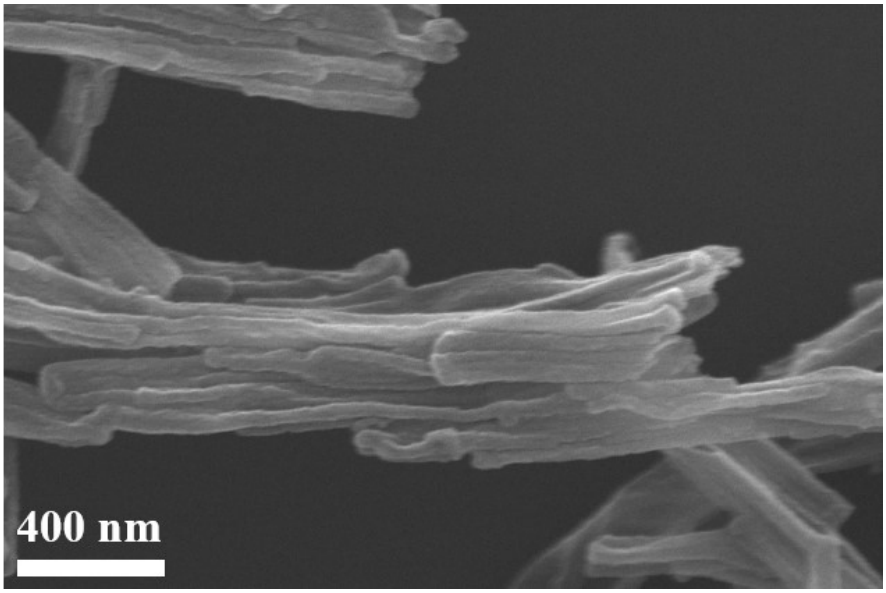

Fig. S5 SEM image of $Fe_4Co_1Ni_2$@hNCTs.

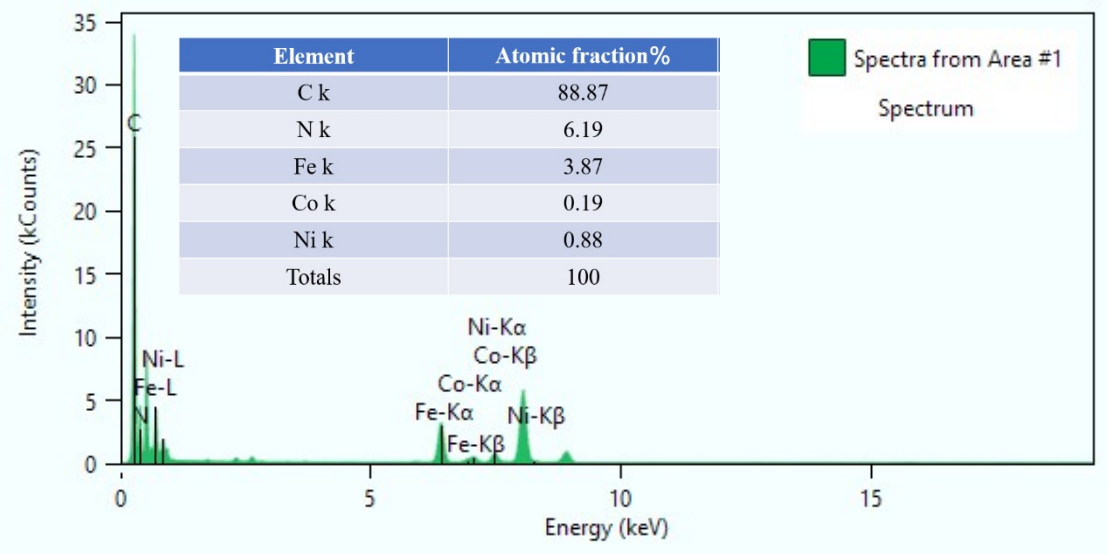

Fig. S6 EDX spectrum of the $Fe_4Co_1Ni_2$@hNCTs.

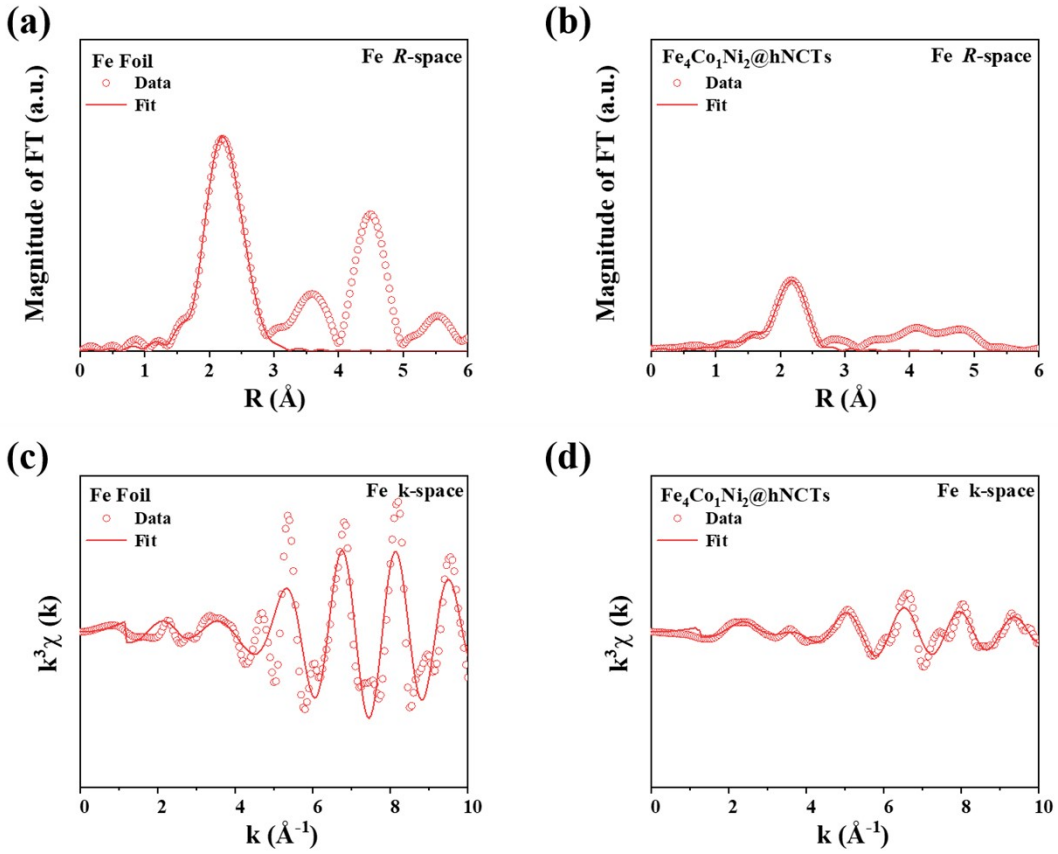

Fig. S7 The FT-EXAFS fitting curve of Fe foil at R-space (a) and k-space (c); The FT-EXAFS fitting curve of $Fe_4Co_1Ni_2$@hNCTs at R-space (b) and k-space (d).

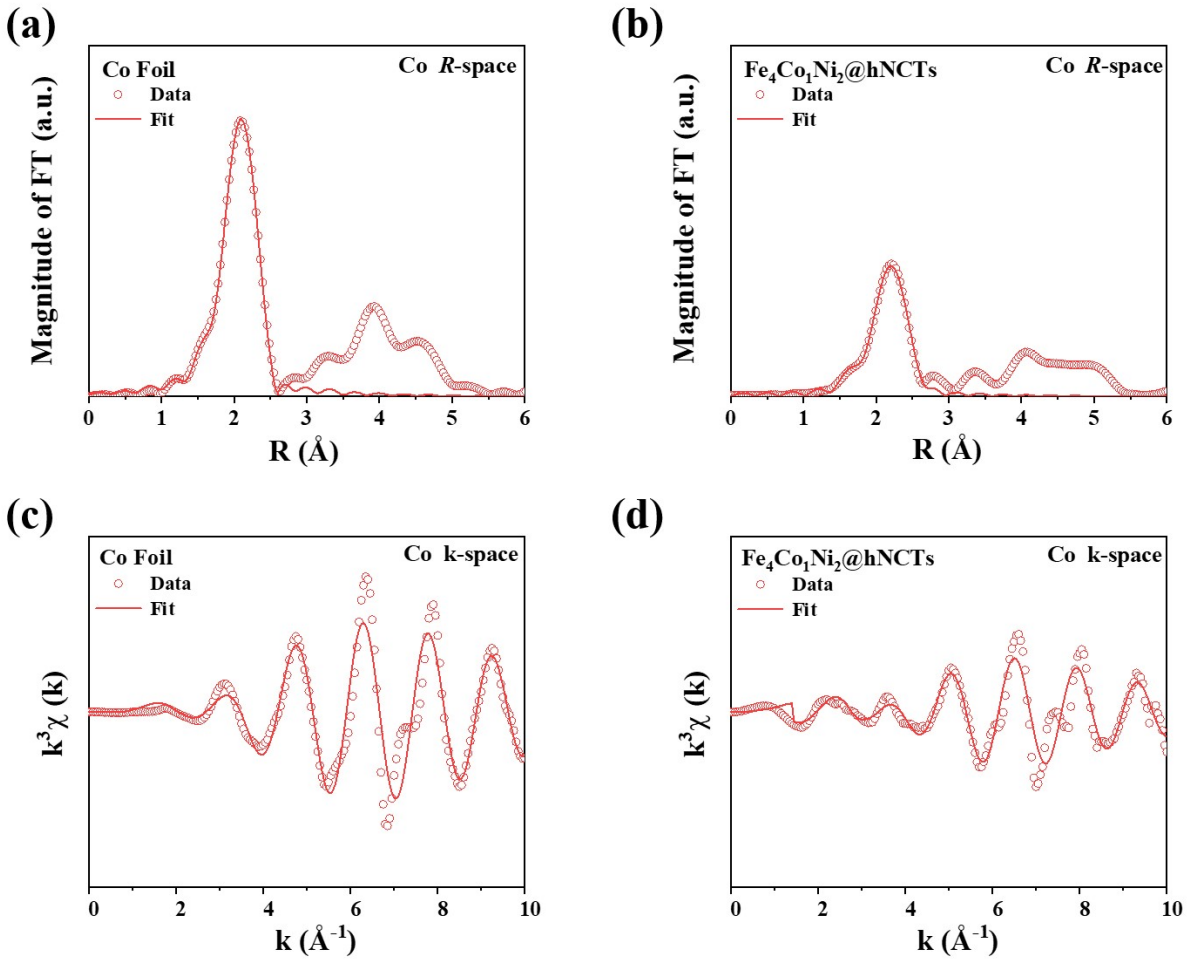

Fig. S8 The FT-EXAFS fitting curve of Co foil at R-space (a) and k-space (c); The FT-EXAFS fitting curve of $Fe_4Co_1Ni_2$@hNCTs at R-space (b) and k-space (d).

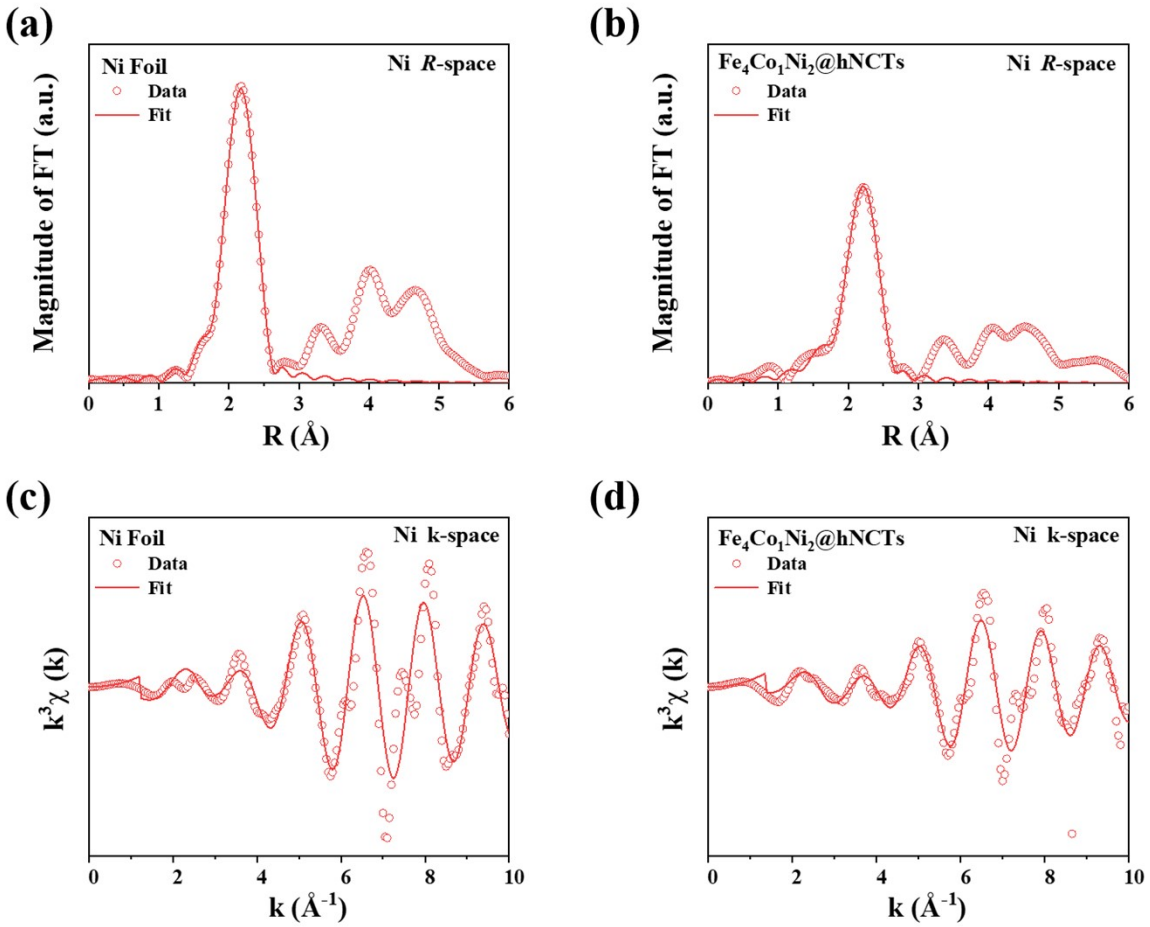

Fig. S9 The FT-EXAFS fitting curve of Ni foil at R-space (a) and k-space (c); The FT-EXAFS fitting curve of $Fe_4Co_1Ni_2$@hNCTs at R-space (b) and k-space (d).

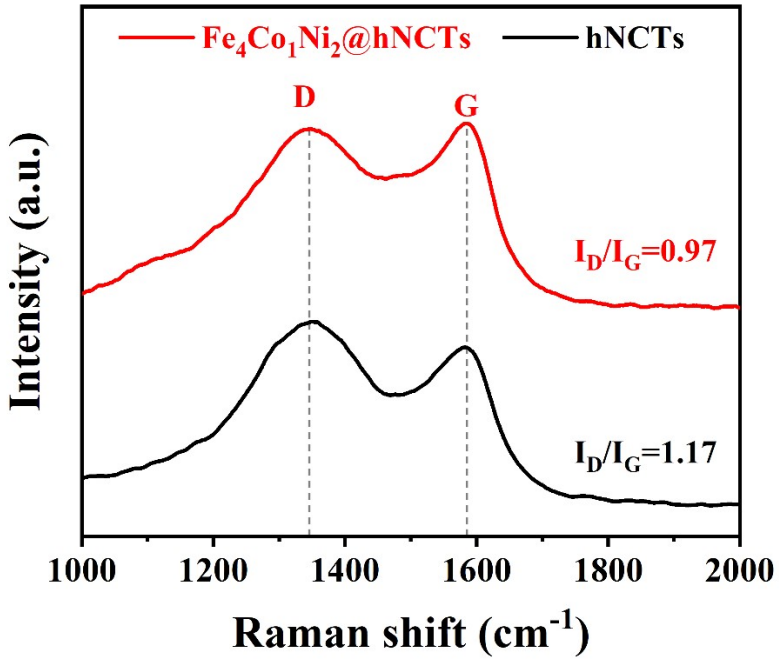

Fig. S10 Raman spectra of $Fe_4Co_1Ni_2$@hNCTs and hNCTs.

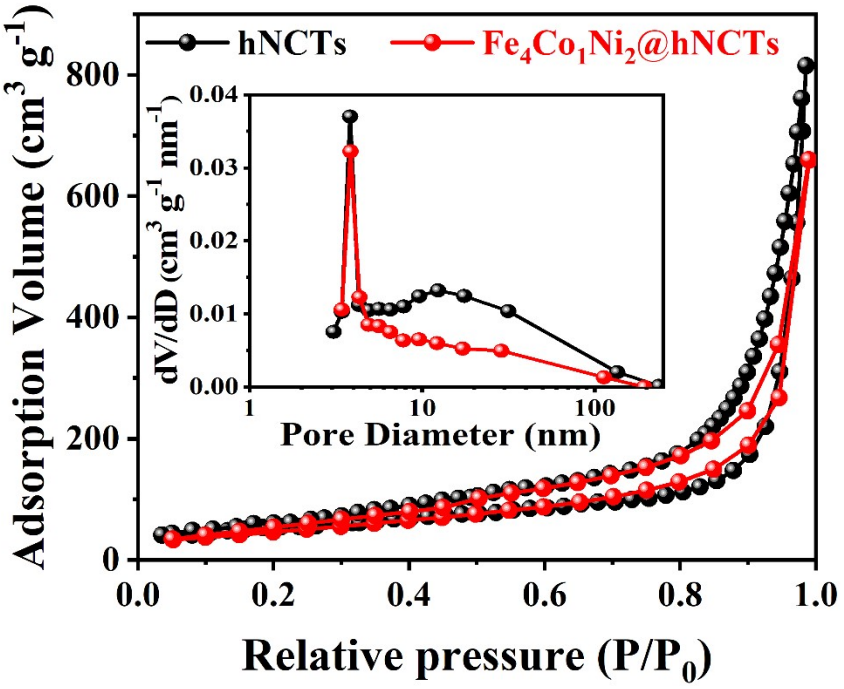

Fig. S11 N_2 adsorption-desorption isotherms (inset is pore size distribution curves) of $Fe_4Co_1Ni_2$@hNCTs and hNCTs.

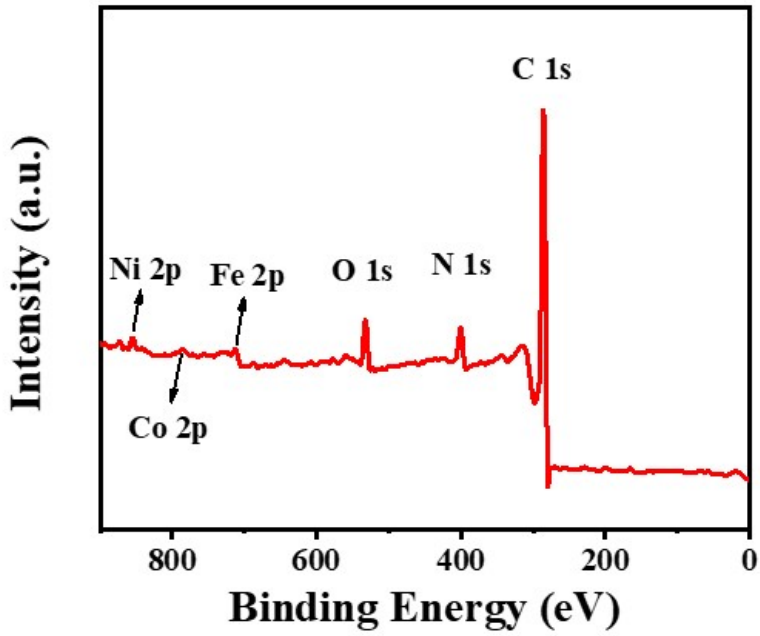

Fig. S12 XPS survey spectra of $Fe_4Co_1Ni_2$@hNCTs.

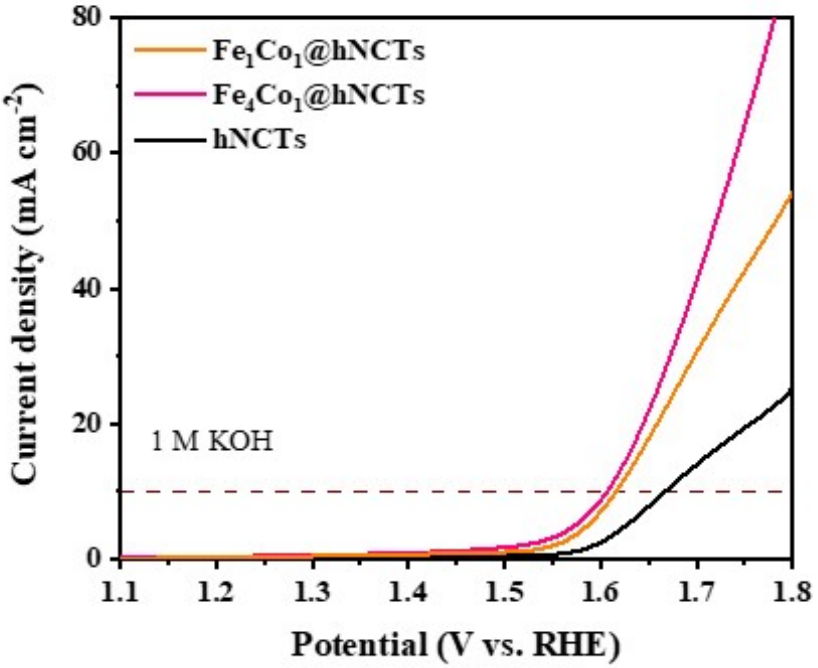

Fig. S13 LSV curves of Fe_4Co_1@hNCTs, Fe_1Co_1@hNCTs and hNCTs in 1.0 M KOH at a scan rate of 10 mV s^{-1}.

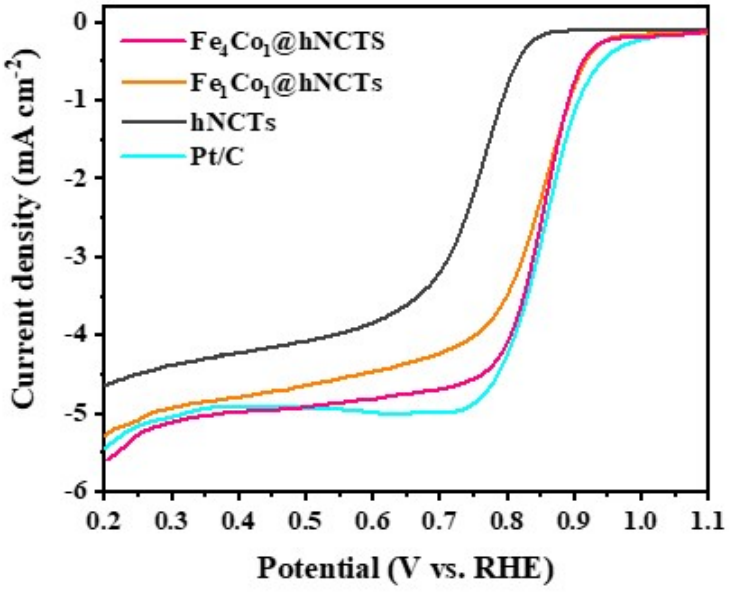

Fig. S14 LSV curves of the ORR in an O_2-saturated 0.1 M KOH solution at the rotation rate of 1600 rpm and a scan rate of 10 mV s^{-1}.

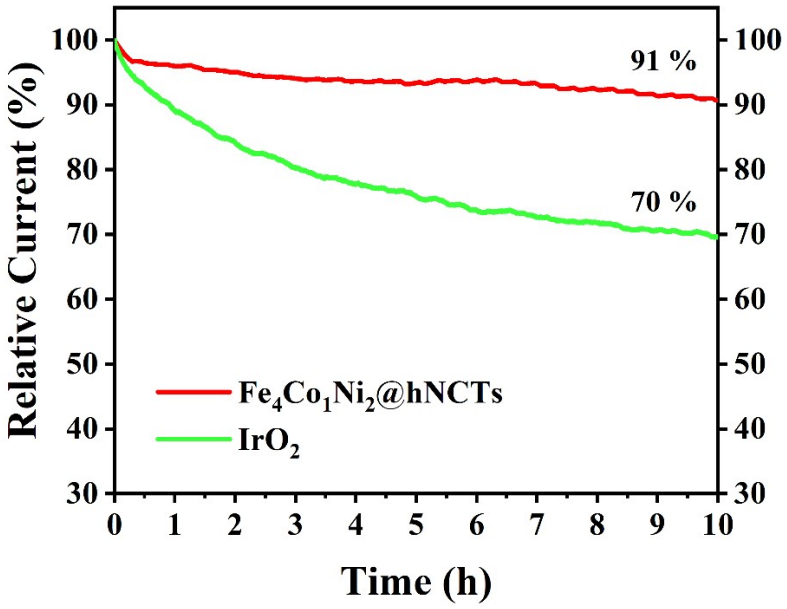

Fig. S15 OER chronoamperometric response of $Fe_4Co_1Ni_2$@hNCTs and IrO_2 at a constant potential of 1.60 V (vs. RHE) in 1.0 M KOH.

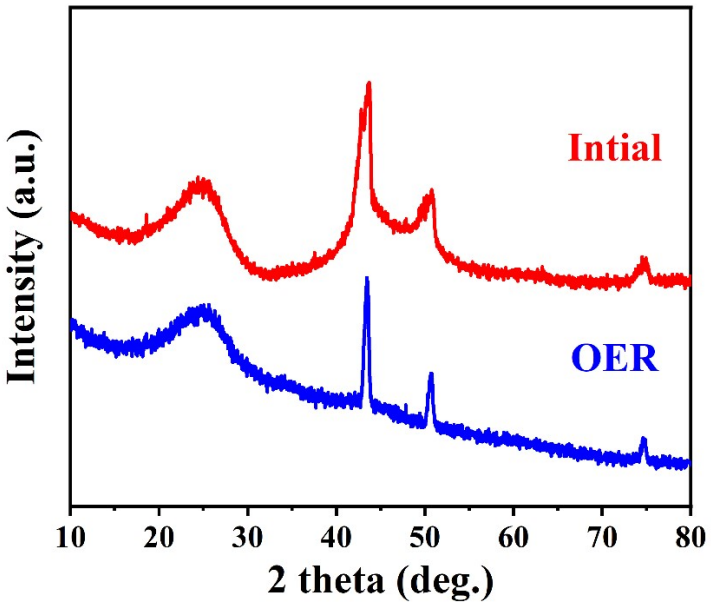

Fig. S16 XRD pattern of $Fe_4Co_1Ni_2$@hNCTs before and after 10 h OER testing.

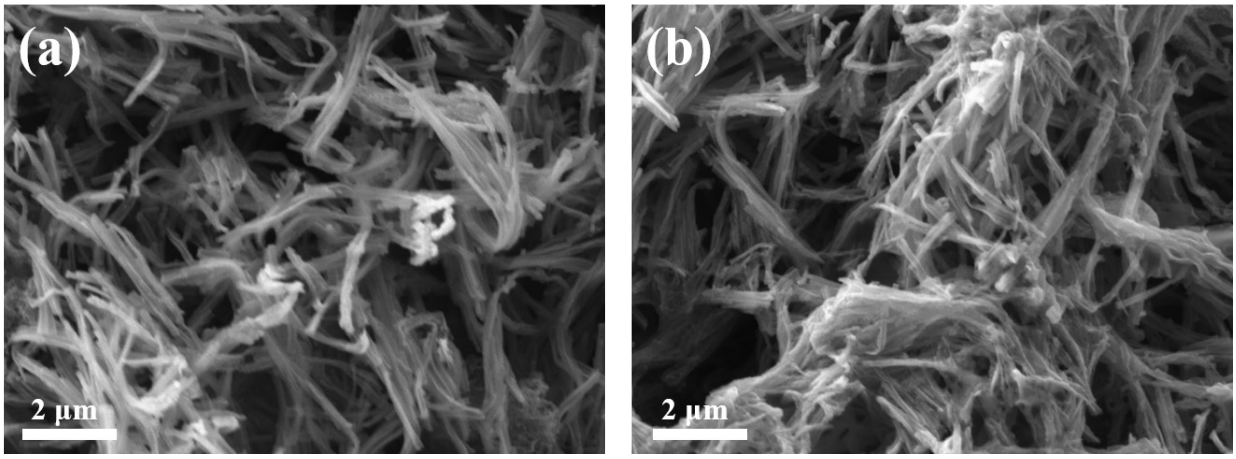

Fig. S17 SEM images of $Fe_4Co_1Ni_2$@hNCTs before (a) and after 10 h OER testing (b).

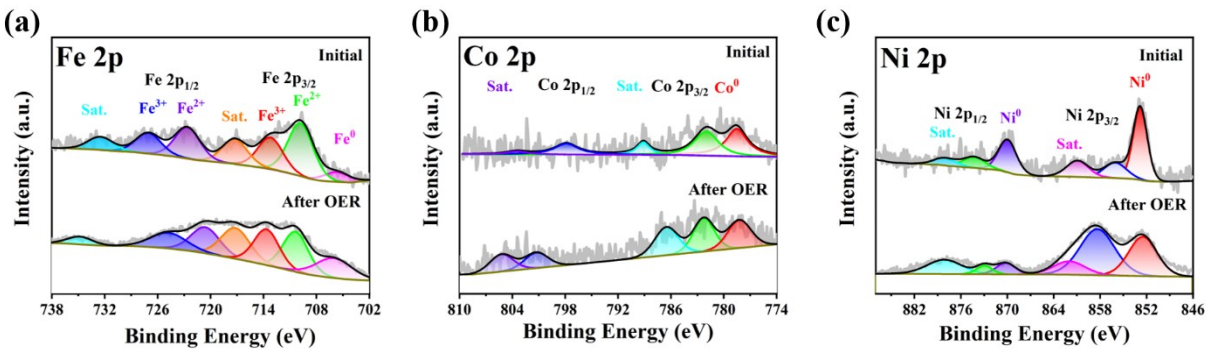

Fig. S18 XPS spectra of a) Fe 2p, b) Co 2p and c) Ni 2p for $Fe_4Co_1Ni_2$@hNCTs after 10 h OER testing.

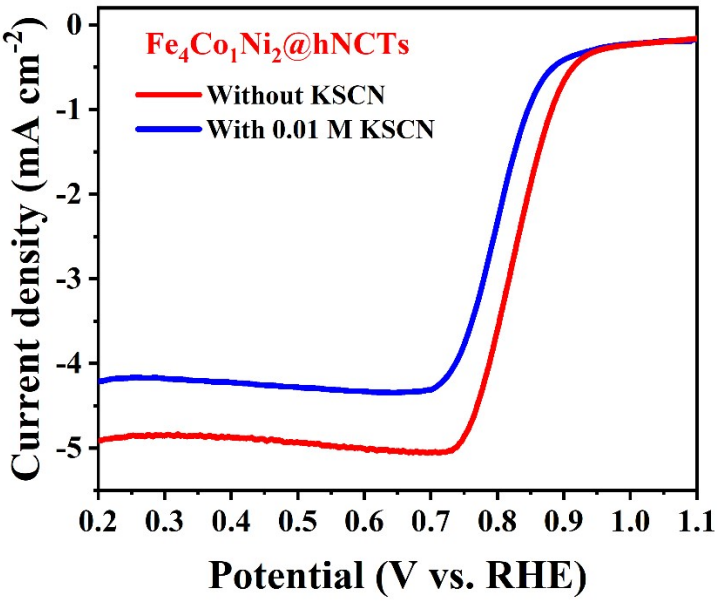

Fig. S19 LSV of $Fe_4Co_1Ni_2$@hNCTs in 0.1 M KOH with and without KSCN.

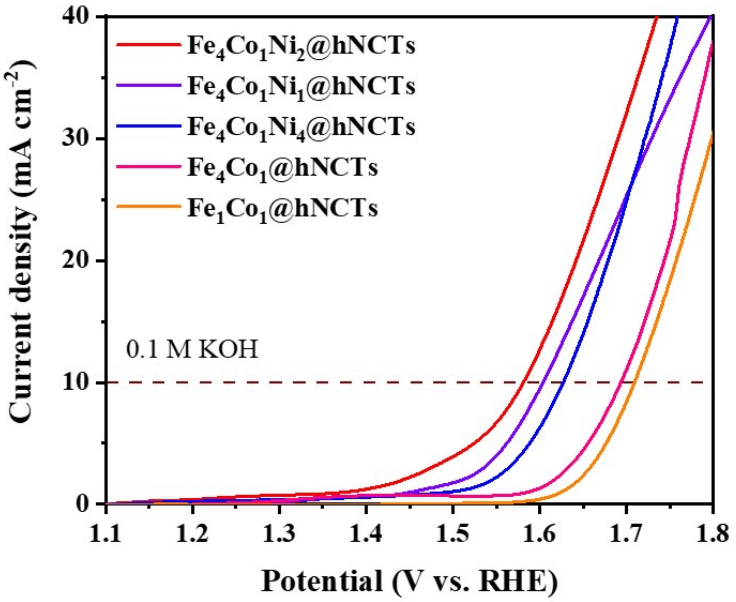

Fig. S20 LSV curves of $Fe_4Co_1Ni_1$@hNCTs, $Fe_4Co_1Ni_2$@hNCTs, $Fe_4Co_1Ni_4$@hNCTs, Fe_4Co_1@hNCTs and Fe_1Co_1@hNCTs in 0.1 M KOH at the rotation rate of 1600 rpm and a scan rate of 10 mV s^{-1}.

2. Supplementary Tables

Table S1. EXAFS fitting parameters at the Co K-edge for various samples（S_0^2=0.679 for Fe, S_0^2=0.696 for Co，S_0^2=0.715 for Ni ）

Sample	Shell	*CN*[a]	*R*(Å)[b]	σ^2(Å^2)[c]	ΔE_0(eV)[d]	*R* factor
Fe Foil	Fe-Fe1	8*	2.46±0.01	0.00481±0.0019	5.36±2.88	0.006
	Fe-Fe2	6*	2.84±0.01	0.00493±0.0029	5.31±4.26	
Fe_2O_3	Fe-O	4.6±1.1	1.97±0.01	0.01±0.004	-6.1±3.2	0.019
	Fe-Fe	4.7±1.0	2.97±0.01	0.006±0.0019	-1.5±1.9	
	Fe-Fe	3.2±1.4	3.44±0.01	0.00006±0.0027	14.1±3.3	

FeO	Fe-O	1.5±0.2	2.14±0.01	0.002±0.001	8.33±1.9	0.018
	Fe-Fe	8.6±1.7	3.03±0.01	0.01±0.002	-0.78±1.8	
Sample Fe	Fe-N	1.2±0.8	1.89±0.01	0.01±0.002	5.16±12.9	0.013
	Fe-Fe	3.0±0.4	2.49±0.01	0.006±0.001	6.37±1.6	
Co foil	Co-Co	12*	2.49±0.01	0.0061±0.0004	-5.9±0.595	0.004
Co_3O_4	Co-O	5.2±0.5	1.91±0.01	0.0025±0.0009	-6.5±1.5	0.006
	Co-Co	3.9±1.1	2.84±0.01	0.0027±0.0015	-7.5±2.5	
	Co-Co	11.7±3.2	3.35±0.01	0.0079±0.002	-7.8±1.8	
Sample Co	Co-N	1.2±0.6	1.96±0.01	0.002±0.008	6.84±13.89	0.009
	Co-Co	6.2±0.4	2.50±0.01	0.007±0.0009	7.81±1.14	
Ni Foil	Ni-Ni	12*	2.48±0.01	0.005±0.0002	0.71±0.02	0.002
NiO	Ni-O	5.5±0.6	2.08±0.01	0.005±0.001	-1.9±1.4	0.003
	Ni-Ni	12.2±1.0	2.94±0.01	0.008±0.0007	-5.1±0.8	
Sample Ni	Ni-N	2.1±1.7	1.93±0.01	0.008±0.01	-6.2±11.1	0.007
	Ni-Ni	6.9±0.6	2.51±0.01	0.006±0.0007	7.3±1.0	

Note: [a]*CN*, coordination number; [b]*R*, distance between absorber and backscatter atoms; [c]σ^2, Debye-Waller factor to account for both thermal and structural disorders; [d]ΔE_0, inner potential correction; *R* factor indicates the goodness of the fit. S_0^2 was fixed to 0.696 for Co, 0.679 for Fe and 0.715 for Ni, according to the experimental EXAFS fit of Co foil, Fe Foil and Ni Foil by fixing CN as the known crystallographic value.

Table S2. Comparison of other reported transition metal-doped electrocatalysts.

	Catalysts	$E_{j=10}$	$E_{1/2}$	Electrolyte	ΔE	Ref
1	$Fe_4Co_1Ni_2$@hNCTs	1.58	0.83	0.1 M KOH	**0.75**	This work
2	Co@hNCTs	1.63	0.87	0.1 M KOH	**0.76**	[1]
3	$Fe_{1.2}$Co@NC/NCNTs	1.585	0.82	0.1 M KOH	**0.765**	[2]
4	C/CoFe-30–650	1.58	0.81	0.1 M KOH	**0.77**	[3]
5	Co/NGC-3	1.626	0.85	0.1 M KOH	**0.776**	[4]
6	Co/HMSC	1.626	0.84	0.1 M KOH	**0.786**	[5]
7	N-CoNi/PCS	1.6	0.8	0.1 M KOH	**0.8**	[6]
8	N-GCNT/$FeCo_3$	1.73	0.92	0.1 M KOH	**0.81**	[7]
9	FeNi-NC	1.64	0.83	0.1 M KOH	**0.81**	[8]
10	CoFe@NCNTs	1.68	0.84	0.1 M KOH	**0.84**	[9]
11	CoNi@N-C	1.73	0.82	0.1 M KOH	**0.91**	[10]

3. Supplementary References

1. Q. Zhou, Z. Zhang, J. Cai, B. Liu, Y. Zhang, X. Gong, X. Sui, A. Yu, L. Zhao and Z. Wang, *Nano Energy*, 2020, **71**, 104592.
2. S. Li, W. Chen, H. Pan, Y. Cao, Z. Jiang, X. Tian, X. Hao, T. Maiyalagan and Z.-J. Jiang, *ACS Sustainable Chemistry & Engineering*, 2019, **7**, 8530-8541.
3. F. Shi, K. Zhu, X. Li, E. Wang, X. Zhu and W. Yang, *Journal of Energy Chemistry*, 2021, **61**, 327-335.
4. J. Li, Y. Kang, D. Liu, Z. Lei and P. Liu, *ACS applied materials & interfaces*, 2020, **12**, 5717-5729.
5. P. Zhu, J. Gao and S. Liu, *J. Power Sources*, 2020, **449**, 227512.
6. L. Chen, Z. Xu, W. Han, Q. Zhang, Z. Bai, Z. Chen, G. Li and X. Wang, *ACS Applied Nano Materials*, 2020, **3**, 1354-1362.
7. C. Y. Su, H. Cheng, W. Li, Z. Q. Liu, N. Li, Z. Hou, F. Q. Bai, H. X. Zhang and T. Y. Ma, *Advanced Energy Materials*, 2017, **7**, 1602420.
8. L. Yang, X. Zeng, D. Wang and D. Cao, *Energy Storage Materials*, 2018, **12**, 277-283.
9. P. Cai, Y. Hong, S. Ci and Z. Wen, *Nanoscale*, 2016, **8**, 20048-20055.
10. H. Ning, G. Li, Y. Chen, K. Zhang, Z. Gong, R. Nie, W. Hu and Q. Xia, *ACS Appl Mater Interfaces*, 2019, **11**, 1957-1968.